

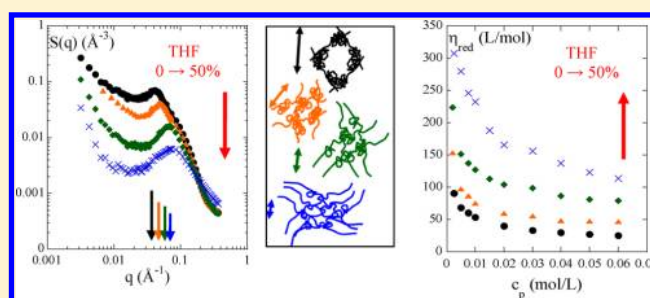
# Behavior of Hydrophobic Polyelectrolyte Solution in Mixed Aqueous/Organic Solvents Revealed by Neutron Scattering and Viscosimetry

Wafa Essafi,<sup>\*,†</sup> Amira Abdelli,<sup>†,‡</sup> Gada Bouajila,<sup>§</sup> and François Boué<sup>\*,||</sup><sup>†</sup>Institut National de Recherche et d'Analyse Physico-Chimique, Pôle Technologique de Sidi Thabet, 2020 Sidi Thabet-Tunisie<sup>‡</sup>Faculté des Sciences de Bizerte, Département de Chimie, 7021 Jarzouna, Bizerte-Tunisie<sup>§</sup>Faculté des Sciences de Tunis, Département de Chimie, 2092 El Manar, Tunis-Tunisie<sup>||</sup>Laboratoire Léon Brillouin, UMR 12 CNRS-IRAMIS CEA Saclay, 91191 Gif sur Yvette Cedex, France

## Supporting Information

**ABSTRACT:** We investigate in this paper the influence of the improvement of the solvent quality on the structure and the viscous properties of solutions of an hydrophobic polyelectrolyte, poly(styrene-*co*-sodium styrenesulfonate): PSS. The solvent used is a mixture of water and an organic solvent, THF, which is also slightly polar. We use small angle neutron scattering in the semidilute regime and viscosimetry as a function of concentration in dilute and semidilute unentangled regime. The structure, namely the scattering from all chains, is characterized by a maximum ("polyelectrolyte peak"). Its position and amplitude depends, at a given sulfonation rate of

PSS, on the solvent quality through the added amount of organic solvent (THF). These evolutions with the THF amount are more pronounced when the sulfonation rate  $f$  is low (more hydrophobic polyelectrolyte) and the amount of added THF is high. Adding THF to hydrophobic PSS ( $f = 0.50$  or  $f = 0.38$ ), diminishes also the "shoulder" visible in the  $\log I - \log q$  plot and associated with the pearl size. It is therefore proposed that when THF is added to aqueous polyelectrolyte solutions, the pearls are dissolved and the chain conformation evolves from the pearl-necklace shape already reported in pure water toward the string-like conformation in pure water for fully sulfonated PSS. An addition of THF also reduces the important low  $q$  upturn found with hydrophobic polyelectrolyte solutions: the large aggregates are dissolved by THF. The upturn can become for PSSNa  $f = 0.38$ , after adding enough THF (50%), even smaller than that for the charged hydrophilic case PSSNa  $f = 0.82$ , in water. This can mean that in the quasi-fully charged PSS at  $f = 0.82$  there are still hydrophobic effects in water, which is disagreeing with our recent reports, or that the electrostatics contribution to the upturn is reduced due to a lower dielectric permittivity. Concerning the hydrophilic polyelectrolyte, poly(sodium-2-acrylamido-2-methylpropanesulfonate)-*co*-(acrylamide): AMAMPS, no evolution in structure occurs until 25% THF. The viscosimetry variation with THF fraction is in good agreement with the scattering one up to 25%: though little dependent on THF for AMAMPS, and for hydrophilic PSSNa, it increases for hydrophobic PSSNa in agreement with the chain expansion signaled by scattering. At 50% THF concentration, the hydrophilic polyelectrolyte shows new surprising behaviors: the scattering of PSSNa is no longer characteristic of polyelectrolytes, and AMAMPS solutions display an unexpected viscosity decrease.



## 1. INTRODUCTION

"Hydrophobic" polyelectrolytes form a very important class of polymers, combining ionizable groups, which dissociate in water into electrostatically charged parts, and hydrophobic parts (being part of the backbone in homopolymers, or one of the repeat units in copolymers, or being grafted to the backbone). This combination opens a huge range of opportunities for properties, exploited in industrial as well as in living worlds. At the first rank is the control of the degree of expansion of the chain under the repulsion between electrostatic charges, and thus the control of several interesting material properties: gel swelling can be cited, but we will be more concerned here with the powerful viscosifying properties (e.g., thickening in paints and cosmetics, enhanced oil

recovery<sup>1–5</sup>). Conversely, when all parts (ionizable or not) of the chains are under good solvent conditions in water, we deal with solvophilic, more precisely here "hydrophilic" polyelectrolytes. For a better control, it is important to understand how the chain expansion, or more precisely the chain conformation, makes the properties just listed arise. To monitor the latter, we will work on a very well-known hydrophobic polyelectrolyte, partially sulfonated polystyrene, the solution structure of which is easy to study by radiation scattering,<sup>6</sup> and has the advantage of being satisfyingly theorized by the pearl necklace model.<sup>7–10</sup>

Received: July 16, 2012

Revised: September 21, 2012



Among the macroscopic properties, as said, we will focus on viscosity using basic measurements. So we will be able to check, through structural data input, the theories of viscosity<sup>11,12</sup> which will gain being investigated in more detail, because they are well-known to deserve more understanding. Although both kinds of data, scattering and viscosity, are available in the literature, they have been rarely acquired systematically on the same polymer, as done in this paper, with a well-defined system. This enables us to observe a new effect, the increase of viscosity with addition, under a given quantity, of organic solvent, which is able to dissolve the hydrophobic parts of the polyelectrolyte, and to relate this effect to the dissolution of the pearls which is monitored by small angle neutron scattering.

Let us recall the general background about polyelectrolytes chain conformation and interactions in a solvent, e.g., water. Let us start with the **dilute regime**. For hydrophilic polyelectrolytes the single chain is theoretically described as an extended rodlike configuration of electrostatic blobs,<sup>13–15</sup> whereas for hydrophobic polyelectrolytes, the single chain is described in the framework of the pearl-necklace model.<sup>7–10</sup> The balance between collapse and extension results in the formation of compact beads (the pearls) joined by narrow elongated strings, in agreement with simulations.<sup>16–20</sup> Experimental results have been reviewed in different papers, like in our former one,<sup>21</sup> especially on scattering measurements. Our group of authors addressed the pearl necklace model using partially sulfonated polystyrene. The actual chain chemical structure is slightly different from the theoretical situation because it is a random copolymer of two different segments, ionizable hydrophilic ones (sulfonated) and hydrophobic ones (not sulfonated). It was shown by SAXS that the initially wormlike chains collapse into more compact objects, further from each other.<sup>22–24</sup> It was proposed that the low internal dielectric constant  $\epsilon^{25}$  inside the pearls leads to counterion/polyion pairs, explaining the reduction in osmotic pressure.<sup>26</sup> Another group, using addition to water of miscible bad solvent (or marginal), acetone, showed that the polyelectrolyte chain undergoes a coil to globule collapse transition.<sup>27,28</sup> A third system dealt with specifically interacting alkaline earth cations which can neutralize anionic chains.<sup>29,30</sup>

In the **semidilute regime**, where many chains interact with each other, i.e.,  $c_p > c_p^*$  ( $c_p^*$  is defined as the concentration above which the volume occupied by each chain overlaps the one occupied by the neighbor chains;  $c_p^*$  depends on the average size of the chains just before overlapping;  $c_p^*$  is the order of  $M/(4/3\pi R^3)$ , where  $R$  is the chain size and  $M$  its molecular weight), the highly charged polyelectrolytes in good solvent are theoretically described by the isotropic model in which the chains are interpenetrated and form an isotropic transient network of mesh  $\xi$ .<sup>13,14</sup> The polyelectrolyte chain is still a random walk of correlation blobs of size  $\xi$ , each one being an extended configuration of electrostatic blobs. In the case of **hydrophilic polyelectrolyte**,  $\xi$  scales with polyelectrolyte concentration as  $c_p^{-1/2}$ ,<sup>13,14</sup> as early verified by SANS<sup>31–33</sup> and SAXS<sup>34</sup> for highly charged chains, and also for partial charge rates  $f$ .<sup>35</sup> There is also a predicted scaling of  $\xi$  with  $f$ , which can be extended to account for Oosawa–Manning<sup>36,37</sup> counterion condensation, as shown through SANS.<sup>38</sup> In the case of a **hydrophobic polyelectrolyte**, two regimes are predicted by Dobrynin et al.:<sup>9,10</sup> the string controlled regime, similar to the one observed in the hydrophilic case ( $\xi \sim c_p^{-1/2}$ ,  $\xi > l_{str}$ ), the string length between two neighboring beads), and

the bead-controlled regime  $\xi \sim c_p^{-1/3}$ ,<sup>9,10</sup> where the system behaves as a solution of charged beads of constant size.

Experimentally, in such a semidilute regime this time, the scattering comes from scatterers of two different chains, when all chains have the same contrast with the solvent. The **total structure function**  $S_T(q)$ , measured by SAXS or SANS, displays a maximum at a  $q = 2\pi/\xi$ ; it was found that  $\xi$  scales as  $c_p^{-\alpha < 0.4}$  when the chemical charge fraction  $f$  decreases,<sup>24,39</sup> as seen later through SAXS and atomic force microscopy studies.<sup>40,41</sup> The counterion condensation was shown larger than for the hydrophilic case:<sup>36,37</sup> the effective charge is strongly reduced,<sup>26</sup> as explained recently.<sup>42</sup> Another method of labeling, zero average contrast (ZAC) using both nondeuterated and deuterated chains enables us to **measure** directly the intrachain scattering  $S_1(q)$ . Totally sulfonated polystyrene shows a wormlike chain conformation,<sup>43</sup> whereas partially sulfonated PSS showed a composite strings and pearls conformation,<sup>39</sup> in good agreement with the pearl-necklace model and with recent simulations.<sup>20</sup> The size of the pearls is several nm and increases when the rate  $f$  of sulfonation, or chemical charge, decreases.

Other measurements concern polymers deposited from a solution onto a surface using ellipsometry<sup>23</sup> and AFM, on different polycations<sup>44,45</sup> and more recently partially sulfonated polystyrene in AFM liquid cell.<sup>46</sup>

Concerning the effect of the solvent quality, as for dilute solutions, it can be (i) **decreased** using solvent mixtures (water plus acetone<sup>27,28</sup>), leading to two regimes of  $\xi \sim c_p^{-\alpha}$  with two  $\alpha$  being  $-1/2$  and  $-1/7$ ,<sup>47</sup> in qualitative agreement with the pearl necklace model as in dilute regime. It can be **increased**:

- (ii) by increasing the temperature<sup>48,21</sup> on sulfonated PSSNa at intermediate charge rate, showing a temperature effect consistent with a shift on  $\Theta$  temperature,
- (iii) by using a polar organic good solvent<sup>47,6</sup> DMSO with PSS, resulting in a classical polyelectrolyte-like behavior, both for the value  $\alpha = -1/2$  and for the form factor measured by ZAC,<sup>6</sup>
- or (iv) by adding to water a low proportion of THF, an organic good solvent for the polyelectrolyte backbone, miscible with water:<sup>6</sup> the solution structure evolved upon THF addition toward the hydrophilic behavior.<sup>6</sup>

In the present paper, we try to make use of such good knowledge of the solution structure to relate it with macroscopic properties; here we consider the viscosity properties, in dilute regime. The reduced viscosity  $\eta_{red}$  (L/mol) data can be analyzed according to the empirical Fuoss equation:<sup>49</sup>

$$\eta_{red} = \frac{A}{(1 + P c_p^{0.5})} \quad (1)$$

According to various theoretical calculations, for a polyelectrolyte of a given molecular weight, the ratio  $A/P$  of the Fuoss equation parameters directly reflects the number of effective charges per chain  $Z$ . In the Witten–Pincus approach,  $A/P \sim Z^2$ , whereas in the Rabin approach,  $A/P \sim Z$ . Galin et al.<sup>50</sup> measured the reduced viscosity  $\eta_{red}$  of polyelectrolytes in some various solvents; they found a large range of values of  $A/P$ , from very low to as high as for fully charged polyelectrolyte in water and associated them with a “polyelectrolyte character”, namely a rate of charge  $f$ . SAXS measurements<sup>47</sup> were conducted on the same systems. More recently, viscometry was also conducted in parallel with structural measurements in

the case of the effect of temperature on hydrophobic partially sulfonated polystyrene (PSS) solutions.<sup>21</sup>

In the present work, we also associate the two techniques, on a system that allows very accurate control in both cases: we investigate solutions of the hydrophobic partially sulfonated polystyrene (at different charge rates but always above the Manning-condensation threshold in water), in a mixture of water and THF, both by:

- small angle neutron scattering measurements in the semidilute regime and thus we determine the total structure function of the solution,
- viscosimetry in more dilute solutions, pertaining to the dilute or semidilute unentangled regime.

The behavior of the hydrophobic polyelectrolyte will be compared to that of poly(sodium 2-acrylamido-2-methylpropanesulfonate)-*co*-(acrylamide): AMAMPS, which is a completely hydrophilic polyelectrolyte in good solvent (water) at the same intermediate rate of sulfonation.

## II. MATERIAL

**II-1. Polymer Synthesis and Characterization.** The hydrophobic polyelectrolyte used in this study is a copolymer of styrene and sodium styrene sulfonate (PSSNa) (poly(sodium styrenesulfonate)<sub>*f*</sub>-(styrene)<sub>1-*f*</sub>) whose chemical structure is shown on Figure 1. It was prepared by

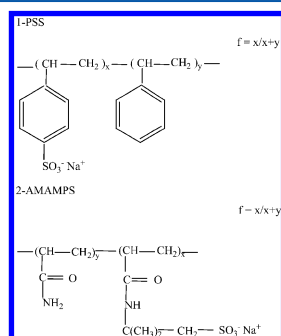


**Figure 1.** Chemical structure of the polyelectrolytes used in this work. *f* is the degree of sulfonation.

postsulfonation of polystyrene ( $M_w = 280\,000$  g/mol of batch no. 16311DB of Sigma-Aldrich Reference182427) based on the Makowski procedure,<sup>24,51</sup> which enables partial sulfonation and leads to a well-defined polyelectrolyte.<sup>52</sup> The rate of sulfonation *f* of the polyelectrolytes was varied between 0.35 (the limit for solubility in water) and 1 (fully charged). The rate of sulfonation *f* is thus always above the Manning condensation limit for the chemical rate, equal to  $a/l_B \sim 0.35$  for PSS in water (*a*, length of one unit,  $l_B \sim e^2/(\epsilon kT) \sim 7$  Å, Bjerrum length in water).

The hydrophilic polyelectrolyte also studied in this paper is (poly(sodium-2-acrylamido-2-methylpropanesulfonate)<sub>*f*</sub> -*co*-(acrylamide)<sub>(1-*f*)</sub>), whose chemical structure is shown in Figure 1. The average molar mass of the repeat unit is  $71 + 158f$ . It was synthesized by radical copolymerisation of acrylamide with 2-acrylamido-2-methylpropanesulfonic acid, a method reported formerly<sup>53</sup> which was slightly modified by adjusting the ratio of the two monomers to obtain, after neutralization, a fraction of ionizable unit (AMPS), *f*, between 0.35 and 1. Thus these chains are also highly charged polyelectrolytes. The resulting molecular weight is  $M_w = 650\,000$  g/mol ( $N_w = 2838$ ) and the

polydispersity is 2.6, for *f* = 1. Note that both polyelectrolytes (AMAMPS and PSS) are salts of strong acid, bearing  $\text{SO}_3^-$  anions as side groups when ionized, with  $\text{Na}^+$  counterions. So the two polyelectrolytes used in this study differ mainly by the solvation characteristics of their backbone (hydrophobic in the case of PSS, hydrophilic in the case of AMAMPS).

**II-2. Preparation of Solutions.** The organic solvent chosen to be added to water is tetrahydrofuran (THF), which is partly polar because its dielectric constant  $\epsilon$  is 7.6, and it dissolves the backbone, i.e., pure polystyrene (not sulfonated) as well as the partially sulfonated PSS for rates  $f \leq 0.6$  at a polymer concentration of 0.34 mol/L. Concerning the hydrophilic polyelectrolyte AMAMPS, it is not dissolved by pure THF whatever the charge content at a polymer concentration of 0.34 mol/L. However, below 50% of THF in water all polymers should be completely soluble.

For the SANS measurements, solutions were prepared by dissolving the dry polyelectrolyte in  $\text{D}_2\text{O}$  (used as delivered from Eurisotop) or in the mixture  $\text{D}_2\text{O}$ /deuterated THF and letting at rest for two days before measurements.

For viscosity measurements, dry polyelectrolyte was dissolved in deionized  $\text{H}_2\text{O}$ . After 2 days, the solutions were filtered with a hydrophilic syringe filter of 5  $\mu\text{m}$  porosity. For the case of solvent mixture, THF is added after the solution filtering and the mixture is let under stirring for 2 h before measurement. Each solution was kept about 5 min in the bath prior to the measurements, for temperature equilibrium.

All concentrations are expressed in mol/L of the corresponding monomer.

**II-3. SANS Measurements.** Small angle neutron scattering (SANS) measurements were performed on the PACE spectrometer at the Orphée reactor of LLB, CEA-Saclay, France ([www-llb.cea.fr](http://www-llb.cea.fr)).

A range of scattering vector  $q = (4\pi/\lambda) \sin(\theta/2)$  between 0.003 and 0.36  $\text{\AA}^{-1}$  was covered by using the following three settings:  $D = 1$  m -  $\lambda = 6$  Å,  $D = 4.7$  m -  $\lambda = 13.2$  Å, and  $D = 4.7$  m -  $\lambda = 6$  Å. The scattered intensity was recorded by a multidetector with 30 concentric, 1 cm wide rings. The response of each ring was normalized to the (flat) incoherent scattering of light water. Samples were contained in 2 mm thick quartz cells.

All measurements were done at room temperature. The cells were capped and sealed to prevent THF evaporation; the level of the liquid was checked.

The recorded intensity was corrected for sample thickness, transmission, incoherent and background scattering (the solvent contribution). Using direct beam measurements of Cotton method,<sup>54</sup> the intensities were obtained in absolute units of cross-section ( $\text{cm}^{-1}$ ); they were then divided by the contrast factor,  $k_H^2$ , where  $k_H$  (cm or Å) =  $(b_H - b_s(V_{\text{molecular,H}}/V_{\text{molecular,S}}))$ .  $b_H$  ( $b_s$ ) is the scattering length of the non-deuterated average repeat unit H (respectively for S, of the  $\text{D}_2\text{O}$  solvent molecule). The unit is therefore the one of the inverse of a volume. The SANS data are plotted as  $S(q)$  ( $\text{\AA}^{-3}$ ) versus  $q$  ( $\text{\AA}^{-1}$ ).

**II-4. Viscosity Measurements.** Viscometric measurements of the polyelectrolyte solutions were carried out with a micro Ubbelohde tube of 0.53 mm diameter by using a SCHOTT viscometer (AVS 470).

### III. RESULTS

The expected improvement of the solvent quality for the hydrophobic polyelectrolyte solutions was followed by means of two techniques: SANS and viscosimetry.

**III-1. Small Angle Neutron Scattering Study in the Semidilute Regime.** The organic solvent THF was added to aqueous polyelectrolyte solutions until 50%.

In what follows, we note “% THF” the percentage by volume of THF in the solvent mixture.

**III-1-a. Effect on a Hydrophilic Polyelectrolyte.** The SANS profiles showing the effect on structure of THF addition for the hydrophilic polyelectrolyte p(AMPS)  $f = 1$  are presented in Figure 2. The polyelectrolyte concentration is kept equal to

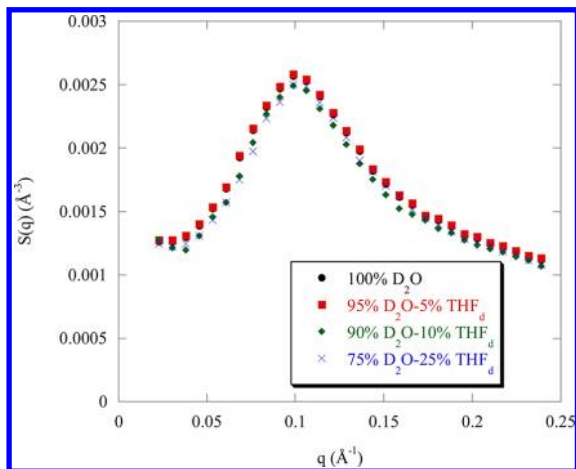


**Figure 2.** Evolution at medium  $q$  of the SANS profiles with the percentage of added THF to aqueous solutions of p(AMPS)  $f = 1$ . The polyelectrolyte concentration  $c_p = 0.34$  mol/L.

0.34 mol/L; thus we are always in the semidilute regime, for all solvent compositions. The number of units per chain is  $\sim 2838$ , the monomer size is about  $2.5$  Å; the effective charge is therefore close to  $f_{\text{eff}} = a/l_B = 0.35$ . The fully extended length is  $L \sim 2838 \times 2.5 = 7095$  Å. At the present ionic strength,  $L_p$  is of the order of  $50$  Å,  $R_g = [LL_p/6]^{1/2} \approx 243$  Å, which gives  $c_p^* \approx M_w/(^{4/3}\pi R_g^3) \sim 0.0188$  g/cm<sup>3</sup>. This  $c_p^*$  value is much lower than the concentration at which we worked:  $c_p = 0.0779$  g/cm<sup>3</sup>.

It emerges that the scattering function is independent of THF addition, in shape and in intensity. Namely, the position of the peak is unchanged as well as its intensity, and the scattered intensity at the minimum  $q$  explored is constant with THF addition, at least up to a value of 25% THF (i.e., still with a majority of water), indicating that the solvent quality is neither improved nor abated.

**III-1-b. Effect on a Hydrophobic Polyelectrolyte.** In what follows, we investigate the SANS profiles over a wide range of scattering vector  $q$  as a function of THF addition in the PSS solutions, for the three chemical charge rates. We try to make the best use of the  $\log I - \log q$  representation. The polyelectrolyte concentration is kept equal to  $0.34$  mol/L for all solvent compositions. To estimate  $c_p^*$ , we use the expression  $c_p^* \approx M_w/(^{4/3}\pi R_g^3)$ , which requires the knowledge of  $R_g$ .  $R_g$  was measured by Spiteri et al.<sup>39</sup> for PSSNa  $f = 0.36$ ,  $M_{1,w} = 90$  000 g/mol and it was found equal to  $76 \text{ Å} \pm 3 \text{ Å}$ . In that case, the overlap concentration was equal to  $c_{p,1}^* = M_{1,w}/(^{4/3}\pi R_g^3) = 0.0811$  g/cm<sup>3</sup>. We start from this value and correct for the

dependence of  $c_{p,1}^*$  over the molecular weight according to Dobrynin et al (eq 25 of ref 14),  $c_p^* \approx M_w^{-2}(B/a)^3$ .

In our case, the molecular weight is much larger,  $M_{2,w} = 380$  000 g/mol, which gives  $c_{p,2}^* = c_{p,1}^* M_{1,w}^2/M_{2,w}^2 = 0.0045$  g/cm<sup>3</sup>. This  $c_{p,2}^*$  value is ten times lower than the concentration at which we worked:  $c_p = 0.0482$  g/cm<sup>3</sup>. For higher charge  $f$ , as well as after THF addition, the chain is more extended, hence  $c_p^*$  is necessarily lower than  $c_{p,2}^*$ . Thus all solutions are in the semidilute regime.

For  $f = 0.82$  (Figure 3), there is a tiny effect of addition of 5% THF: the abscissa of the peak is shifted to large  $q$ 's, its intensity

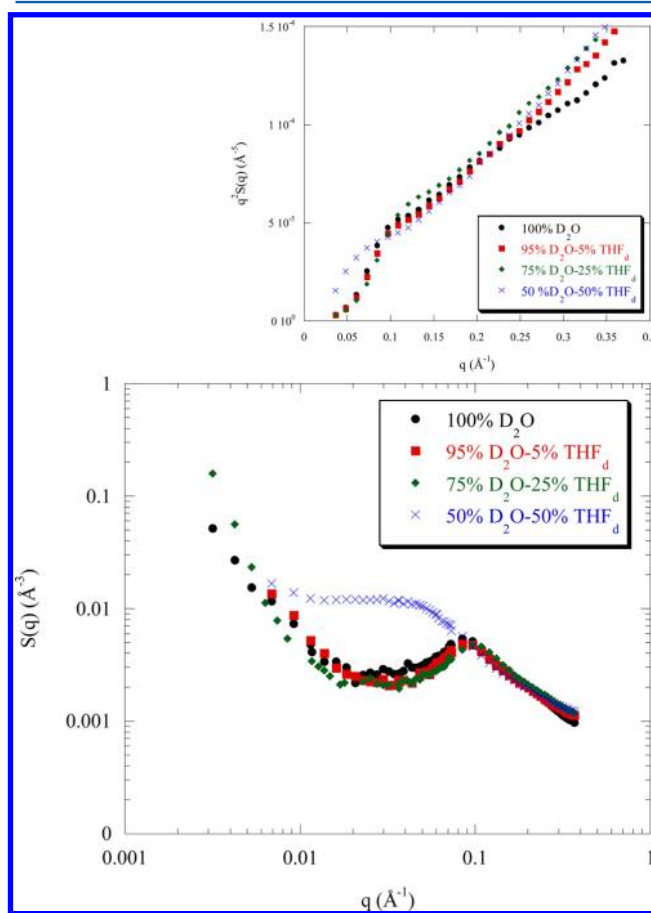


**Figure 3.** Evolution of the SANS profiles with the percentage of added THF to aqueous solutions of PSSNa  $f = 0.82$ . The polyelectrolyte concentration  $c_p = 0.34$  mol/L. The inset represents the Kratky plot of the intensity scattered by the same solutions.

is decreased a little, its width is reduced; also the minimum corresponding to the flat part region is lowered. The same slight evolution is continued when 25% THF is added. Our interpretation is that the foot of the low  $q$  upturn influences the region of the minimum, including the aspect of the peak. It is then possible that THF lowers the value of the foot because the polymer was therefore still slightly hydrophobic in water ( $f$  is smaller than one). However, at the lowest  $q$  values, the upturn scattering varies in an erratic way and we cannot conclude in this range.

Finally, for 50% THF added, surprisingly, we observe a complete change of behavior, although the appearance of the solution remains the same, i.e., crystal clear: the peak is replaced by a plateau, the scattering at low  $q$  is as important as in a neutral polymer solution, the decay at large  $q$  is steeper than in

the case of the three other solvent compositions (0%, 5%, and 25% THF), signaling less extended scattering objects, i.e., parts of the polyelectrolyte chains that are less extended than in the case of the other solvent compositions (0%, 5%, and 25% THF). These two facts suggest straight away that the polymer is neutral. Let us be quantitative: the signal in log–log plot can be described by a plateau at low  $q$  followed by a straight line slope of  $-1.5$  at intermediate  $q$ , which itself followed by a second slope of  $-1$  at large  $q$  (see Figure SI 4 in Supporting Information). The large  $q$  slope  $-1$  may suggest a rodlike conformation at short scale due to some specific local interactions which we will not comment further. The crossover between the 1.5 slope and the low  $q$  plateau is qualitatively close to the one in the scattering from a neutral polymer semidilute solution (the large  $q$  slope being  $q^{-1.6}$ ). Let us be more quantitative: in our case the intersection between the plateau and the  $q^{-1.5}$  straight line occurs around  $q = 0.045 \text{ \AA}^{-1}$ . For comparison, the crossover obtained in the scattering from a neutral polystyrene semidilute solution<sup>55</sup> occurs at  $q^* = 0.055 c_p^{3/4}$  ( $c_p$  in  $\text{g}/\text{cm}^3$ ); taking the same molarity (and therefore similar volume fraction,  $c_p = 3.5 \times 10^{-2} \text{ g}/\text{cm}^3$ ), we find also  $q^* = 0.045 \text{ \AA}^{-1}$ . It is not the purpose of this paper to make a more detailed analysis, but we conclude that the structure at low  $q$  is therefore close to a neutral semidilute solution.

For the more hydrophobic chains,  $f = 0.50$  (Figure 4) and even more for  $f = 0.38$  (Figure 5), the structure strongly varies

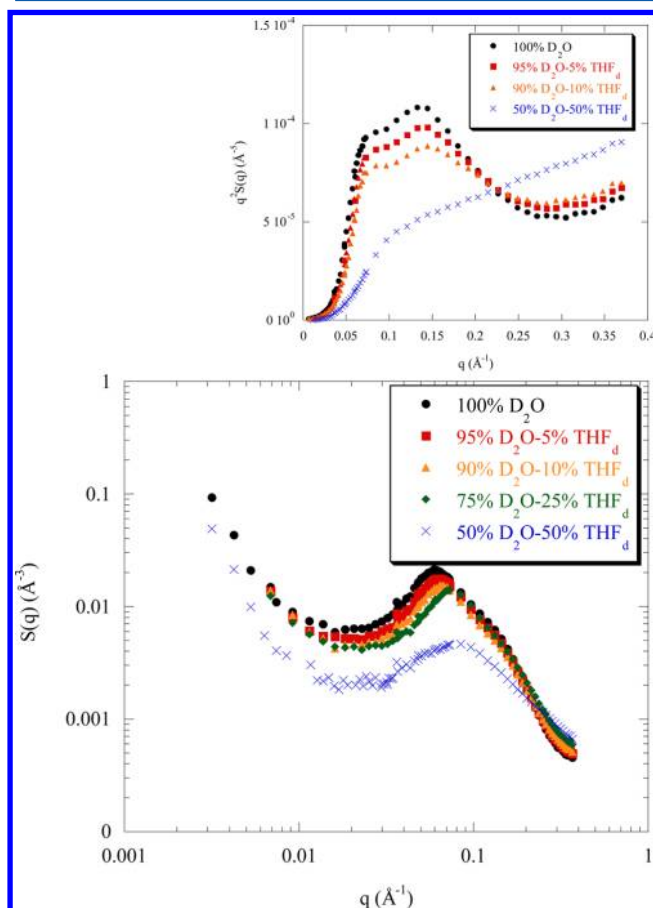


**Figure 4.** Evolution of the SANS profiles with the percentage of added THF to aqueous solutions of PSSNa  $f = 0.50$ . The polyelectrolyte concentration  $c_p = 0.34 \text{ mol/L}$ . The inset represents the Kratky plot of the intensity scattered by the same solutions.

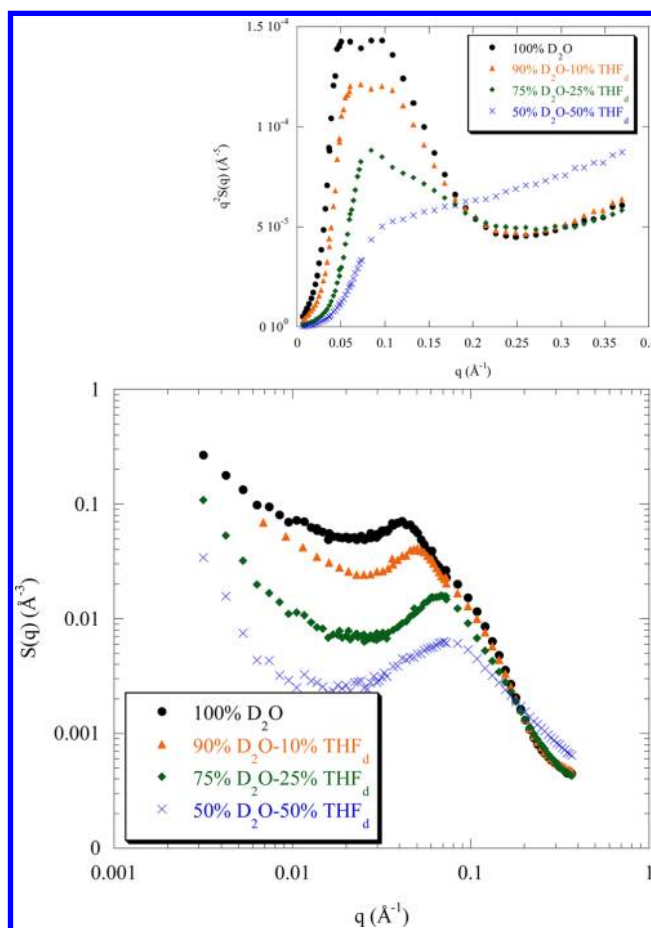


**Figure 5.** Evolution of the SANS profiles with the percentage of added THF to aqueous solutions of PSSNa  $f = 0.38$ . The polyelectrolyte concentration  $c_p = 0.34 \text{ mol/L}$ . The inset represents the Kratky plot of the intensity scattered by the same solutions.

when THF is added. Note that these solutions become more transparent after THF addition until 50%. The peak position  $q^*$  increases and its height decreases. Also, the peak widens: when passing from 0% to 25% THF,  $\Delta q/q^*$  increases from 0.52 to 0.57, for  $f = 0.50$  and from 0.46 to 0.60 for  $f = 0.38$ . Recall that the peak width is related to order degree of the system (the sharper the higher order;  $q^*$  and  $\Delta q$  are determined within uncertainty due to the low  $q$  upturn).

At the right of the maximum we notice, in absence of THF, a shoulder. As earlier commented,<sup>24,39</sup> this is due to the scattering from compact small objects, which are the pearls. When THF is added, this shoulder (see the inset in Figure 5) and the peak are reduced; this effect is more important for  $f = 0.38$  than for  $f = 0.50$  (see the inset in Figure 4). We also observe a slight shift of the shoulder to larger  $q$  with lower slope. Note that even if the disappearance of the shoulder should reduce its apparent width, the widening of the peak, due to less ordered fluctuations, is dominant. For  $f = 0.82$ , this shoulder is absent (see the inset in Figure 3), indicating the absence of pearls. When 50% THF is added, the shoulder vanishes completely and all scattering profiles return to the one of the “hydrophilic case”  $f = 0.82$  in pure water although some small differences remain (see also Figure SI 5 in Supporting Information).

For the low  $q$  region, changes are also noticeable: for  $f = 0.38$ , the upturn at  $q \rightarrow 0$ , much stronger than for  $f = 0.82$  in water,

decreases considerably with THF addition. As a result, on the right of the foot of the upturn, the plateau part widens progressively. The plateau height also lowers: we recover the value for  $f = 0.82$  in water, whereas the upturn foot is shifted to significantly lower  $q$ . The same is true for  $f = 0.5$  (the plateau height is even a bit lower).

In summary of section III-1-b, for the **hydrophobic** polyelectrolyte in the semidilute regime, for  $f = 0.5$  and  $0.38$ , the main trend is that the structure function varies with THF addition suggesting that the solvent quality is improved. This evolution is more pronounced for lower  $f$ . The essential effect, and the most important, is that the scattering from hydrophilic PSS ( $f = 0.82$ ) is recovered with large THF addition, with surprising exception of the case  $f = 0.82 - 50\%$  THF, for which we come close to the behavior of a neutral chain.

We recall that, for the case of  $f = 0.82$  which is close to a **hydrophilic** polyelectrolyte, adding THF at a fraction of 50% has a different effect: it suppresses the polyelectrolyte character of the chain which behaves as neutral.

**III-2. Viscometric Study in the Dilute and Semidilute Unentangled Regimes.** *III-2-a. Hydrophilic Polyelectrolyte.* The variation of the reduced viscosity versus the concentration of AMAMPS  $f = 0.46$  in different mixtures of water/THF, is presented in Figure 6. For all solvent compositions, the curves

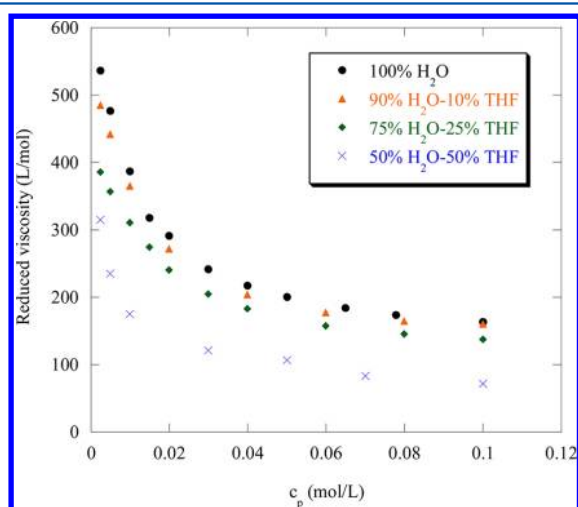


**Figure 6.** Evolution of the reduced viscosity versus the polyelectrolyte concentration, for AMAMPS  $f = 0.46$ , for different solvent compositions of water/THF at 25 °C.

show a polyelectrolyte behavior, namely a typical upturn of the reduced viscosity  $\eta_{\text{red}} = f(c_p)$  at low concentrations. The usual explanation is the following: when the polyelectrolyte concentration decreases, the screening (due mostly to the free counterions) is reduced: the range of the intramolecular repulsion (the Debye length) is increased. Thus the polyelectrolyte chain becomes more extended and  $\eta_{\text{red}}$  increases.<sup>49,56</sup>

With THF addition, we see in Figure 6, at a given concentration of AMAMPS (choosing the example of  $f = 0.46$ ), that the reduced viscosity decreases when THF is added. The effect of THF addition is progressive up to 25%; surprisingly, when a fraction of 50% is reached, the viscosity drops much deeper by about a factor 2. We will return to this particular effect in the Discussion.

*III-2-b. Hydrophobic Polyelectrolyte.* The effect of THF addition on the viscosity of the PSSNa hydrophobic polyelectrolyte aqueous solutions at 25 °C, is shown in Figure 7.

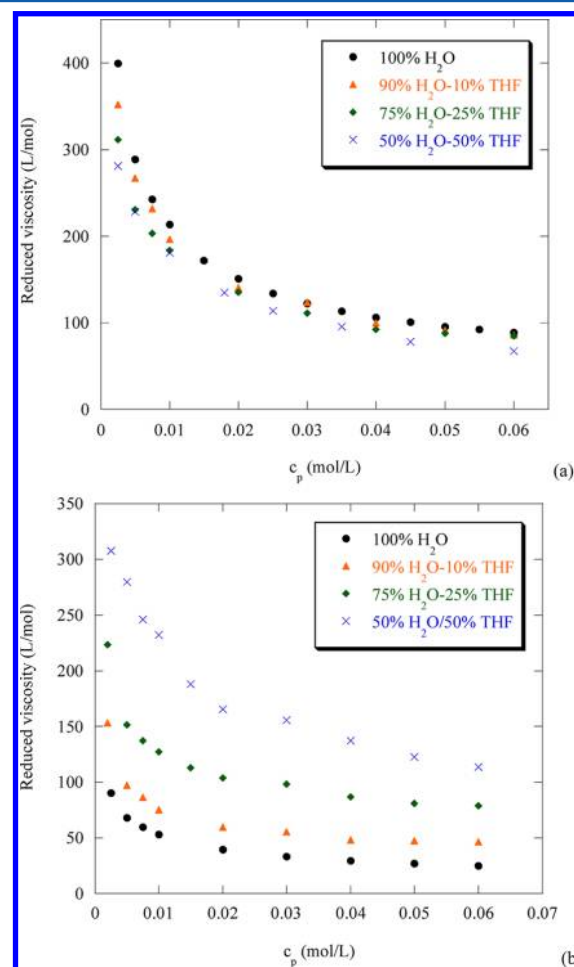


**Figure 7.** Evolution of the reduced viscosity versus the polyelectrolyte concentration, of PSSNa for different solvent compositions of water/THF at 25 °C: (a) PSSNa  $f = 0.75$ ; (b) PSSNa  $f = 0.38$ .

For the two extreme charge fractions, the PSSNa presents the typical polyelectrolyte behavior, like for AMAMPS: the reduced viscosity increases as the concentration decreases. The explanation is the same as given for AMAMPS.

When THF is added, the evolution is different for the two  $f$ 's. For the highly charged PSSNa  $f = 0.75$ , Figure 7a shows that the reduced viscosity decreases as the percentage of THF increases. This is the same effect as for AMAMPS: PSSNa  $f = 0.75$  behaves as a hydrophilic polyelectrolyte. The effect of viscosity reduction is, however, less pronounced than for AMAMPS; this is probably due to the balance with an opposite effect, which we see clearly for a larger hydrophobicity, namely for PSSNa  $f = 0.38$ : in this case the reduced viscosity now *increases* with THF addition. What increases here must be the hydrodynamic volume of the chain. It can be attributed to an improvement of the solvent quality.

In summary of the Results, when the polyelectrolyte has a clear-cut hydrophobic character in water, viscosimetry as well as scattering suggest an increase of the polyelectrolyte character with THF addition.

## IV. DISCUSSION

**IV-1. Small Angle Neutron Scattering Study in the Semidilute Regime.** *IV-1-a. Effect of Added THF on a Hydrophilic Polyelectrolyte. Qualitative Aspects.* Concerning the hydrophilic polyelectrolyte, p(AMPS)  $f = 1$ , it emerges first from data that the scattering is independent of THF addition, at least up to 25% (no data for 50%). The curves for 0%, 5%, 10%, and 25% THF just overlap. These results are in agreement with previous results<sup>6</sup> obtained by X-ray scattering where the contrast comes mainly from the condensed counterions on the polyelectrolyte chain (whereas here for neutron scattering the contrast comes from the units of the polyelectrolyte chain itself). This means that the polyelectrolyte chain network of the AMAMPS has its mesh size and degree of order unchanged, and that the effective charge remains constant with THF addition. Finally, the constancy of the scattered intensity at the lowest  $q$  value available ( $2 \times 10^{-2} \text{ \AA}^{-1}$ ) also suggests that the effective charge is constant, assuming  $S(q \rightarrow 0) \sim 1/f_{\text{eff}}$  (see eq 2 below). This is a slight contradiction with Manning condensation, which is expected to hold  $f_{\text{eff}}$  at the value  $a/l_B$ , which should vary here, because it implies  $1/l_B \sim \epsilon$ : hence the variation of  $\epsilon$  is not seen in this available  $q$  range. We now propose a more accurate discussion using an analytical expression of  $S(q)$ , just below.

*Analytical Expression of the Scattering.* The expression of the scattering displays several regimes of  $q$ : first, as said above, the scattered intensity at zero angle is related to the osmotic compressibility as, according to the Dobrynin model:<sup>14</sup>

$$S(q \rightarrow 0) = kTc_p \frac{\partial c_p}{\partial \Pi} = \frac{\Phi_p}{f_{\text{eff}} V_{\text{molecular}}} \quad (2)$$

where  $\Phi_p$  is the polymer volume fraction,  $V_{\text{molecular}}$  is the molecular volume of the PSS<sup>-</sup>,  $V_{\text{molecular}} = V_{\text{Molar}}/N_{\text{Avogadro}}$  and  $V_{\text{Molar}}$  is the PSS<sup>-</sup> molar volume.

For most of polyelectrolyte solutions, measurements at lower  $q$  are perturbed by a low  $q$  upturn generally observed. Hence such low  $q$ 's have not been explored here for AMAMPS (a slightly lower  $q$  range is explored in Figure 2 of ref 6) and we cannot discuss further for this polymer.

An analytical expression is also available for the dependence of the position of the maximum in the scattering intensity  $q^*$  as predicted by the theoretical models of the semidilute polyelectrolyte solutions derived from the isotropic phase model (de Gennes et al.<sup>13</sup>) by Dobrynin et al.<sup>14</sup> for polyelectrolytes in *good solvents*, therefore far from the  $\Theta$  temperature. The segment length is  $a$ . The chain is a random walk of correlation blobs of size  $\xi$ , each of which is an extended configuration of electrostatic blobs of  $g_e$  monomers inside the blob diameter  $D$ . Therefore,  $\xi$  is close to a geometrical distance between rodlike strands of chains and depends on their effective linear density of segments ( $g_e/D$ ), which we will define as equal to  $B/a$ , defining  $B$  as in ref 14:

$$\xi \propto \left( \frac{B}{c_p a} \right)^{1/2} \quad (3)$$

Let us first assume AMAMPS is in a poor solvent. Equation 3 can be extended to such case. If we stay in the string-controlled regime,  $q^*$  will still be related to the inverse blob size, which now depends on the distance to the theta temperature  $\Theta$  ( $B$  turns out to characterize the solvent quality):

$$q^* \propto \left( \frac{2\pi}{\xi} \right) \propto \left( \frac{(\Theta - T)}{\Theta} \right)^{-1/4} c_p^{1/2} \propto \left( \frac{\tau}{a^2 f_{\text{eff}}} \right)^{-1/4} c_p^{1/2} \quad (4a)$$

for  $T < \Theta$

with  $\tau = (\Theta - T)/\Theta$ , so that:

$$q^* \propto \tau^{-1/4} (\epsilon T)^{1/4} c_p^{1/2} \quad \text{for } T < \Theta \quad (4b)$$

using  $f_{\text{eff}} = (a/l_B) \sim (\epsilon kT/\epsilon^2)$ . If the addition of THF was decreasing the solvent quality for AMAMPS so that  $\tau$  increases, we should observe that  $q^*$  decreases. This is not the case. The constancy of  $q^*$  suggests therefore that water plus THF remains a good solvent for AMAMPS up to 25%.

Thus we consider now the case of *good solvent* ( $T \gg \Theta$ ):  $g_e$  and  $D$  are determined by the fact that the total electrostatic energy between charges inside the electrostatic blob is  $\sim k_B T$ , due to thermal agitation with no influence of the distance to theta and using again  $f_{\text{eff}} = a/l_B$ ,  $q^*$  writes now:

$$q^* \propto \left( \frac{2\pi}{\xi} \right) \propto \left( \frac{B}{c_p a} \right)^{-1/2} \propto \left( \frac{l_B}{a} \right)^{1/7} f_{\text{eff}}^{2/7} (c_p a)^{1/2} \propto l_B^{-1/7} \propto \epsilon^{1/7} \quad T \gg \Theta \quad (5)$$

which does not depend on  $\tau$  (the solvent quality). However, following eq 5, the addition of THF should decrease the dielectric constant  $\epsilon$  and consequently decrease  $q^*$ . This gives a weak theoretical dependence:  $\epsilon^{-1/7}$ . Following a quasi-linear variation of  $\epsilon$ ,<sup>57</sup> the addition to water of 25% THF ( $\epsilon_{\text{THF}} \sim 7.6$ ) is expected to give a decrease of  $\epsilon$  from 78.5 to 58.5. This would change  $q^*$  by less than 4%. Note that the variation of  $S(q^*)$  would be stronger, because it can be expressed by:<sup>13</sup>

$$S(q^*) = S\left(\frac{2\pi}{\xi}\right) \approx g \approx c_p \xi^3 \approx q^{*3} \quad (6)$$

( $g$  is the number of monomer inside the blob  $\xi$ ). This leads to:

$$S(q^*) \propto f_{\text{eff}}^{-6/7} l_B^{-3/7} c_p^{-1/2} \propto l_B^{3/7} c_p^{-1/2} \propto \epsilon^{-3/7} c_p^{-1/2} \quad T \gg \Theta \quad (7)$$

The variation would become about 10% for  $S(q^*)$ : in practice, we do not observe any variation of  $S(q^*)$  either. A possible explanation is that the electrostatic blob picture does not apply here on AMAMPS because the blob size  $\xi_e$  becomes comparable to the segment size  $a$ . We also cannot exclude the possibility that the effects of  $\tau$  (when in conditions of eq 4a and eq 4b, if THF improves solvent quality,  $\Theta$  decreases therefore  $\tau$  decreases and  $q^*$  increases) and  $\epsilon$  compensate each other. However, the fact that such compensation is successful for all THF contents would be surprising.

For addition of 50% THF, we have no available scattering data which would confirm that we are still in good solvent. We only know, from macroscopic visual investigation, that AMAMPS solutions are crystal clear; AMAMPS seems perfectly soluble in 50% D<sub>2</sub>O/50% THF<sub>d</sub> at this polyelectrolyte concentration of 0.34 mol/L. Whatever the state of dissociation of the charges, the solution is not macroscopically destabilized.

*IV-1-b. Effect of Added THF on a Hydrophobic Polyelectrolyte.*

*Qualitative Aspects.* As described in the Results, the evolution of the profiles with adding THF is similar to the one in pure water with increasing the charge rate  $f$ . The only

exception is  $f = 0.82$  at 50% THF, to which we will return at the end of this section. Characteristic values at 25% THF for a given  $f$  (0.50 or 0.38) return close to values at the next highest  $f$  (respectively 0.82 or 0.50) at 0% THF. This effect can be seen quantitatively in Figure 8 showing the shift of  $q^*$ , and the decrease of  $S(q^*)$  and  $S(q \rightarrow 0)$ . For  $f = 0.5$  and 0.38 we need up to 50% THF to make  $q^*$  and  $S(q^*)$  equal to the values for  $f = 1$  in water, and we can assume wormlike conformation.<sup>43</sup> For  $f = 0.82$  a slight improvement of the hydrophilic character is noticeable when 5% or 25% THF is added: the peak is slightly shifted to larger  $q$  (Figure 3, see also Figures SI 1a and SI 2a in Supporting Information).

The behavior at the right of the peak ( $q \sim 0.08\text{--}0.1 \text{ \AA}^{-1}$ ) is very interesting: as said in the Results, for intermediate THF fractions, each solution gives a different scattering, depending on the height of the peak but also displaying some difference in the “shoulder” at the right of the peak (Figures 4 and 5). The profile of this shoulder is similar for  $f = 0.5$  and 0.38: there are no obvious differences in slopes. But the whole curve is shifted to lower  $q$  and higher intensity level for  $f = 0.38$ . This is due to the increase in size and volume of the pearls when  $f$  decreases. This shoulder vanishes progressively, which affects the apparent slope of the curve: this can be attributed to the vanishing of the pearl structure. For larger  $f$ , because the pearls are smaller, the shoulder and its decay are visible at larger  $q$ . When THF up to 25% is added, the shoulder height progressively decreases, in all the  $q$  range up to  $0.2 \text{ \AA}^{-1}$ .

If we now look at the Kratky plots, we see some differences for the two rates of charge. For  $f = 0.5$ , the maxima in  $q^2 I(q)$  correspond to the shoulders in the log–log plot. Their abscissa does not vary; hence the pearl size remains constant, while the large  $q$  intensity slightly increases, suggesting that the pearls are less compact. For  $f = 0.38$ , it is clear that the shoulder position increases with THF addition, meaning that the pearl size decreases. The scattering at  $q > 0.2 \text{ \AA}^{-1}$  stays independent of THF addition, meaning that the pearls are still compact. In summary, the response to THF is different when the pearls are larger and more compact. In all cases, the pearls are still present until 25% THF addition.

For 50% THF, for both  $f = 0.38$  and  $f = 0.50$ , the curves get back to the one for  $f = 0.82$  in pure water. So the pearls have vanished, and once they have vanished we do not see any other effect of THF in the size range corresponding to the  $q$  range explored here.

In the low  $q$  region (Figures 4 and 5 and Figures SI 3b, SI 3c in Supporting Information), the scattered intensity at  $q \rightarrow 0$  measured just at the foot of the upturn at  $q \approx 0.0052 \text{ \AA}^{-1}$ , is decreased by THF addition in two ways:

- The value in the “flat part” ( $0.01\text{--}0.05 \text{ \AA}^{-1}$ ) is reached before the low  $q$  upturn is lowered down. If we associate this value with the osmotic compressibility, it suggests that the chains are more charged. The lowest value reached is the same for all  $f$ : this suggests that the chains become completely solvophilic and undergo Manning condensation.
- The upturn at  $q \rightarrow 0$  is also reduced: below 50% THF; this can be interpreted as the reduction of hydrophobicity. But for 50% THF, the upturn for lower  $f$  is still decreased and becomes lower than the one for PSS  $f = 0.82$  in water. In this case hydrophobic interactions could be completely canceled already, and what we observe can be a reduction of the well-known large scale

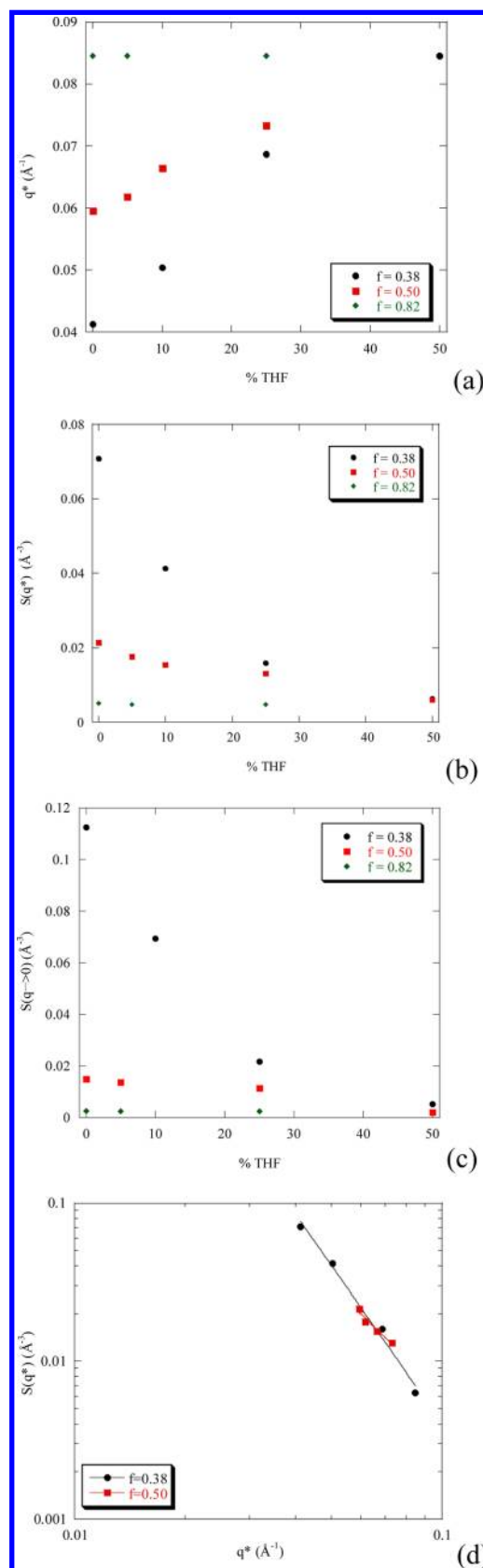


**Figure 8.** Evolution of  $q^*$ ,  $S(q^*)$ , and  $S(q \rightarrow 0)$  as a function of THF addition, and simultaneous evolution of  $S(q^*)$  versus  $q^*$ , for PSSNa at  $c_p = 0.34 \text{ mol/L}$ .

inhomogeneities characteristics of pure polyelectrolyte solutions, attributed to electrostatics.

Let us give an *intermediate qualitative summary*: the addition of THF drives the structural characteristics toward the ones of a more charged, even fully charged, polyelectrolyte in water. This evolution suggests a decrease in size and even disappearance of the pearls size as introduced by the Dobrynin model,<sup>9,14</sup> describing the structure of hydrophobic polyelectrolyte in poor solvent. We now turn to a more quantitative discussion.

**Analytical Expression of the Scattering.** Here we consider directly the case  $T < \Theta$ , which corresponds to the pearl necklace model for PSSNa in water at  $f < 1$ .  $q^*$  is given by eq 4a, where  $q^*$  depends both on  $\varepsilon$  and on the solvent quality (measured by  $\tau$ ). The first parameter is  $\varepsilon$ . Let us consider below an intermediate dielectric constant assuming perfect mixing, although this may be misleading, because water and THF molecules specifically interact with the hydrophilic and hydrophobic regions of the polyelectrolytes. This will be discussed a few paragraphs further below. Returning to the assumption of perfect mixing,  $\varepsilon$  should decrease under THF addition, and as a consequence decrease the effective charge  $f_{\text{eff}}$ , as well as  $q^* \sim \varepsilon^{1/4}$ . This effect of  $\varepsilon$  should be better seen when  $\tau$  is minimal, that is, in the case of PSSNa  $f = 0.82$ . However, results for this value of  $f = 0.82$  deny any direct effect of the variation of  $\varepsilon$ , until 25% of THF. Note that the expected variation is weak ( $\varepsilon^{1/4}$ , i.e., 7.5% for a variation of  $\varepsilon$  from 78 to around 60). For the other  $f$ 's, the variation of  $q^*$  is clearly opposite: it increases which cannot be explained by the effect of  $\varepsilon$ .

We thus turn to the second parameter,  $\tau$ ; its relevance should increase when hydrophobicity increases. This is observed: for  $f = 0.50$  and  $0.38$ , we see a clear difference in the scattering under THF addition, and  $q^*$  increases as predicted,  $q^* \sim \tau^{-1/4}$  (eq 4a).  $\tau = (\Theta - T)/\Theta$  decreases with THF addition. This prompts us to favor the effect of  $\tau$  with respect to  $\varepsilon$  and explain the results as follows: when THF is added to aqueous solutions, the polyelectrolyte tends to behave like a classical polyelectrolyte, because the solvent is better. The THF solubilizes the hydrophobic domains.

**Pearls Features.** This can reduce the pearl size, or the polymer concentration inside the pearls (lower compacity). For  $f = 0.38$  at the right of the peak, the decrease of the shoulder and of the apparent slope at the right of the shoulder, suggest a decrease of the compacity. Conversely, for  $f = 0.5$ , the flattening of the curves and their extent to larger  $q$  strongly suggest a decrease in pearl size. In both cases, the string fraction increases and the chain conformation stretches. Simultaneously, the counterions, initially localized in  $\text{SO}_3^-/\text{Na}^+$  ion pairs inside or condensed at the surface of the pearls, become surrounded by solvent, and dissociate. This increases the effective charge of the chain, although THF is intrinsically less polar.

Concerning the peak height, we can use eq 6, which predicts,  $S(q^*) \approx c_p \varepsilon^3 \approx c_p q^{*-3}$ . Therefore, a direct power law relation should take place between  $q^*$  and  $S(q^*)$ . Indeed, in log–log plot (Figure 8d)  $S(q^*)$  versus  $q^*$  shows a straight line of slope approximately equal to  $-3$ . As a consequence, the variation of  $S(q^*)$  will just reflect the variation of  $q^*$ . On the one hand, the variation should be followed more accurately due to the power 3. On the other hand, however, seen from a technical point of view,  $S(q^*)$  relies more on the conditions of measurement of the scattering and of data treatment (volume, concentration), whereas  $q^*$  is much less dependent on these. In practice, we

observe that the variation of  $S(q^*)$  leads to the same conclusions than the one of  $q^*$ .

**Theta Temperature.** Because we have concluded that  $\tau$  is the relevant parameter, it would be interesting at this stage to give a quantitative estimate of a theta temperature, noted  $\Theta$ , as a function of THF concentration, by extracting  $\tau$  from  $q^*$  using eq 4a. (we neglect small changes in  $\varepsilon$  and  $f_{\text{eff}}$ ). For PSS,  $f = 0.38$ , starting from a value in water  $\Theta = 211^\circ\text{C}$ ,<sup>21</sup> we find that  $\Theta$  decreases importantly and becomes very close to room temperature ( $25^\circ\text{C}$ ) for 25% THF. However, a more accurate account appears difficult using the present experiments only: a more extensive suite of techniques must be used in the future.

**Preferential Sorption.** Only average values of  $\varepsilon$  and  $\tau$  have been considered until now. This could be wrong if preferential sorption of one of the two components of the solvent on the chain occurs. The presence of such adsorption can be discussed allowing to the large  $q$  behavior. First, from the point of view of the SANS technique, this could modify the contrast between chain and solvent. But this is negligible here because deuterated THF and  $\text{D}_2\text{O}$  have similar neutron scattering densities; so the contrast effect is negligible. Second, from the point of view of physicochemistry, preferential adsorption of THF on the hydrophobic domains of the polyelectrolyte chain would result in a more complex solvent local organization, the effect of which is not simple to predict. The simplest assumption is that the hydrophobic domains would be more dissolved than for an homogeneous solvent and surrounded at larger distance by a solvent richer in water. It is difficult to detect any signature of this in the changes of  $S(q)$ . However, we recall that at the largest  $q$ , when pearls have vanished for 50% THF addition, the scattering remains identical to the one for  $f = 0.82$  at all THF contents, indicating an absence of local effect of THF.

**Low  $q$  Scattering.** We end this quantitative Discussion by the scattering at low  $q$ . It can be decomposed in two contributions:

- First, the plateau at the right of the upturn can be identified, following eq 2 to  $S(q \rightarrow 0) = kTc_p(\partial c_p/\partial \Pi) \propto (1/f_{\text{eff}})$ . We observe a decrease with THF suggesting that the effective charge increases, in agreement with ions pairs dissociation or “decondensation”. A difficulty is that the plateau value may be perturbed by the onset of a low  $q$  upturn observed at lower  $q$  (available here only for PSS but not for AMAMPS). With 50% THF, the plateau is better defined because the upturn is reduced and shifted to lower  $q$ .  $S(q \rightarrow 0)$  seems to saturate down to a minimum value, independent of  $f$  and of  $\varepsilon$  (a comparison can be seen in Figure SI 5). However, this measurement is still very inaccurate. To illustrate that, let us compare the measurement value to the predicted one: taking into account all parameters, the predicted expression for  $S(q \rightarrow 0)$ , in  $\text{\AA}^{-3}$ , is exactly eq 2.

$V_{\text{Molar}}$  of the  $\text{PSS}^-$  is known to be close to  $100 \text{ cm}^3$  (assuming all monomers charged), and  $V_{\text{molecular}} = V_{\text{Molar}}/N_{\text{Avogadro}} = 160 \text{ \AA}^3$ . The volume fraction is  $\Phi_p = 0.34 \text{ (mol/L)} \cdot V_{\text{Molar}}/1000 \text{ cm}^3 = 0.034$ . The predicted value is derived in the *Additional Note* before the references, and we find it not far from the measured one. This is because the contribution of the upturn is reduced by THF. It is, however, clear that the measurement is still perturbed by some upturn, even for low  $f$  with 50% THF.

- Second, the upturn contribution: it is attributed to large scale inhomogeneities in the solution (the so-called slow mode in dynamic light scattering), and it is widely

recognized that even hydrophilic polyelectrolyte display low  $q$  upturns, attributed to electrostatics effects. However, here for low  $f$  in pure water ( $f = 0.38$  in particular) the upturn is much higher than for  $f = 1$ . Under THF addition, it decreases: the reason could be that hydrophobic inhomogeneities are a second cause for the upturn and are dissolved by THF. Reciprocally, the lack of THF influence on the lowest  $q$  scattering for  $f = 0.82$  suggests that in this more hydrophilic case these upturns are not due anymore to large hydrophobic aggregates because we would observe that they are dissolved when THF is added. The last fact we have to deal with is the fact that the upturn is less important for  $f = 0.38$  and  $0.50$  at 50% THF addition, than for  $f = 1$  in pure water. This could be due to reduction of  $\epsilon$ , which would agree with the explanation involving electrostatic interactions.

**Summary.** For the hydrophobic polyelectrolyte, the global solvent quality is improved with THF addition and the polyelectrolyte solution adopts a structure characteristic of more charged and elongated chains, like in water for non-hydrophobic polyelectrolyte ( $f = 1$ ). This is due to a decrease of  $\tau$ . We pass from repulsions between collapsed parts of chains behaving as charged spheres, to softer interactions between strands of chains (strings), inside a network of interpenetrated charged chains. Low  $q$  upturns, which are larger for hydrophobic PSSNa (low  $f$ ) in pure water, are abated by THF addition, down to values even lower that for hydrophilic PSSNa in pure water, probably because the dielectric constant is reduced.

For hydrophilic PSSNa, the influence of THF has a similar trend (although very weak) until 25% THF, but reverse when reaching 50%: AT THIS FRACTION, THF lowers the polyelectrolyte character. This is probably due to a decrease of  $\epsilon$ , which reduces charge solvation, while the uncharged segments (polystyrene) remain soluble.

**IV-2. Viscometric Study in the Dilute and Semidilute Unentangled Regimes.** *IV-2-a. Hydrophilic Polyelectrolyte.* The viscosity of polyelectrolyte solutions in semidilute unentangled regime can be described by the evolution of the  $1/\eta_{\text{red}} = f(c_p^{1/2})$ . We will use this representation, which gives often a linear variation in practice; this is the so-called Fuoss law. Though of empirical origin, the Fuoss law<sup>49</sup> (eq 1) is recovered by the theory of Dobrynin et al. for hydrophilic polyelectrolytes<sup>14</sup> and is frequently used to determine the intrinsic viscosity values  $[\eta]$  for polyelectrolytes in aqueous solution, from the intercept of the inverse of the Fuoss representation.

The representation of  $1/\eta_{\text{red}}$  versus  $c_p^{0.5}$ , for the AMAMPS  $f = 0.46$  with the different solvent compositions, gives linear evolutions for all the solvent compositions (Figure 9).

First, consider the intercept  $1/A$  of each of these lines, which gives the inverse of the intrinsic viscosity. The inset in Figure 9 shows that the extrapolated intrinsic viscosity for AMAMPS decreases when THF is added, in a progressive manner from 10% to 50%. This can be explained by a decrease of the dielectric constant of the medium, leading to less charge dissociation, and a reduction of the hydrodynamic radius of the chain.

Second, consider the slope  $P/A$  in Figure 9: it stays identical up to 25% and increases significantly for 50%. According to the theories of Witten<sup>11</sup> and Rabin,<sup>12</sup> the inverse of the slope  $A/P$

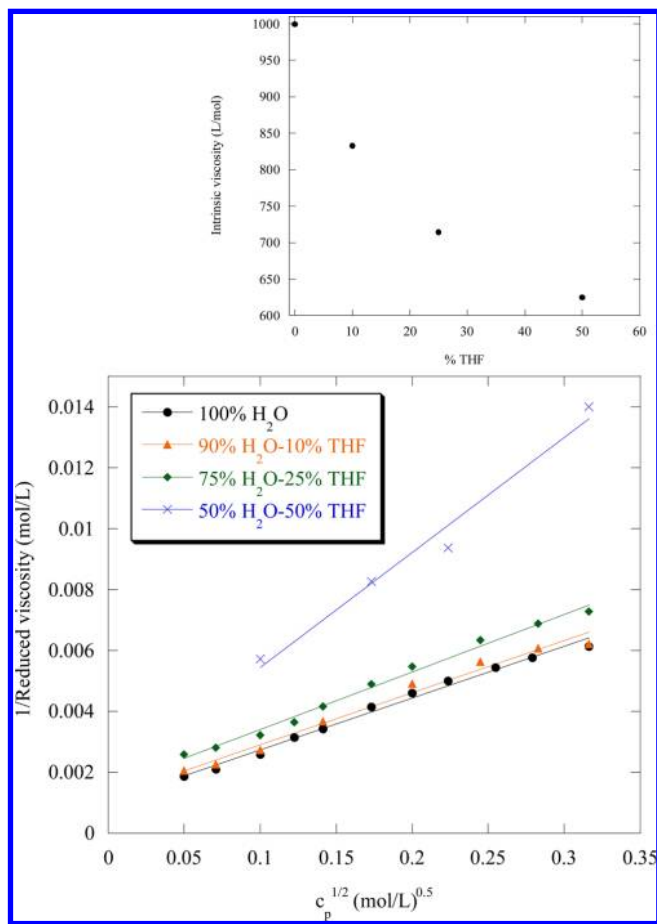


**Figure 9.** Fit of the viscometric data on AMAMPS  $f = 0.46$  at 25 °C as a function of solvent composition with the Fuoss equation. The inset represents the evolution of the extrapolated intrinsic viscosity as a function of solvent compositions.

of the linear evolution of Fuoss directly reflects the number of effective charges per chain  $Z$ . The fact that  $A/P$  decreases as the percentage of THF increases therefore suggests that the effective charge of the polyelectrolyte decreases with THF addition, as already suggested by the intrinsic viscosity, but for  $P/A$  the variation is important only for 50% THF addition.

Finally, let us compare with the evolution under THF addition of SANS: the latter has been measured up to 25% THF added only. The variation of the structure at 25% is tiny, there is only a small reduction of the scattering maximum. Viscosity thus appears more sensitive to THF than SANS. For 50% THF where changes in viscosity are marked both in extrapolated viscosity and in effective charge, we unfortunately have no SANS data to compare. We will compare viscosity and scattering in a similar situation in the case of hydrophilic PSSNa,  $f = 0.82$ , in the next section.

Eventually, our interpretation is that the addition of THF results in a decrease of the dielectric constant  $\epsilon$  of the medium (water/THF).<sup>27,58</sup> This reduces the dissociation of the electrostatic charges along the chain (modification of the Manning condensation threshold  $f_{\text{eff}} = a/l_B$ ), and therefore reduces the viscosity.

*IV-2-b. Hydrophobic Polyelectrolyte.* For the hydrophobic polyelectrolyte, the same usual polyelectrolyte behavior of viscosity with concentration is observed for all PSS charge fractions and all water/THF compositions.

First, the same behavior than for AMAMPS is found at small hydrophobicity for PSSNa  $f = 0.75$ . As seen in Figure 10, the

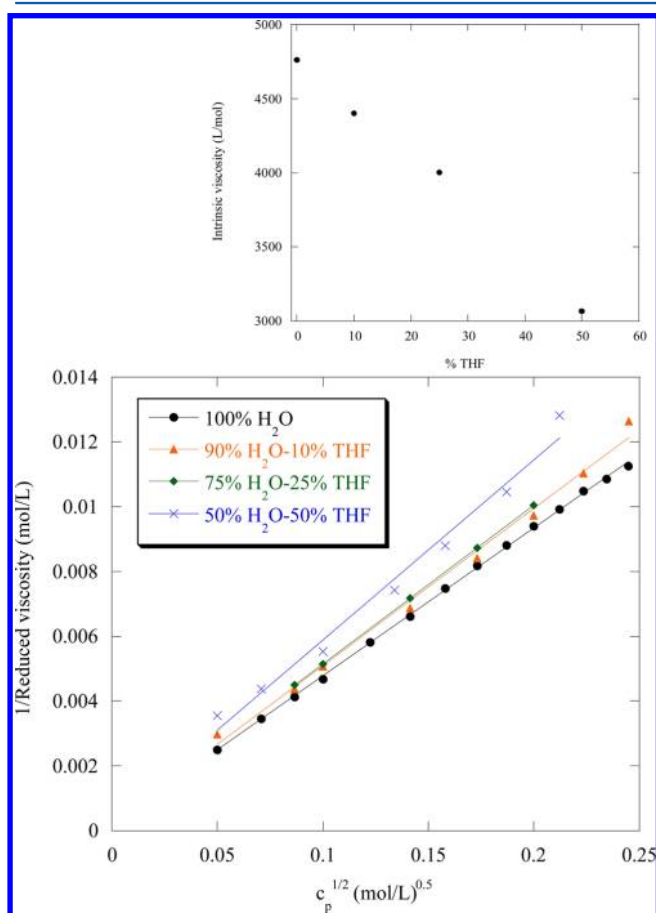


**Figure 10.** Fit of the viscometric data on PSS  $f = 0.75$  at 25 °C as a function of solvent composition with the Fuoss equation. The inset represents the evolution of the extrapolated intrinsic viscosity as a function of solvent composition.

Fuoss law is obeyed;<sup>49</sup> for 10% and 25% THF, as for AMAMPS, the curves lie slightly above the 0% one. The effect is clear-cut for 50% THF. In all cases this is enough to make decrease noticeably the extrapolated intrinsic viscosity when THF is added (inset in Figure 10). We also see on the Figure 10 that the slope of the Fuoss representation increases with THF percentage, slightly until 25% and noticeably for 50%. We attribute this also to the reduction of the dielectric constant of the solvent. Again, according to the theories of Witten<sup>11</sup> and Rabin,<sup>12</sup> this indicates that the effective charge of the polyelectrolyte decreases with THF addition. This can be associated with the *scattering* behavior for  $f = 0.82$  (a value slightly superior to 0.75): for 50% added, the scattering changes completely and loses the usual characteristics of polyelectrolyte (in particular the polyelectrolyte peak vanishes, Figure 3).

Second, the opposite effect is found for lower charge rates and true hydrophobicity (PSSNa  $f = 0.38$ ): the viscosity *increases with THF addition*. In other words, the hydrodynamic volume of the PSSNa increases with the percentage of THF. Fuoss law<sup>49</sup> well fits the experimental results (Figure 11). The extracted intrinsic viscosity increases with THF addition (see the inset in Figure 11). Moreover, the slope of the Fuoss representation decreases as the percentage of THF increases. Still, using the theories of Witten<sup>11</sup> and Rabin,<sup>12</sup> we deduce this

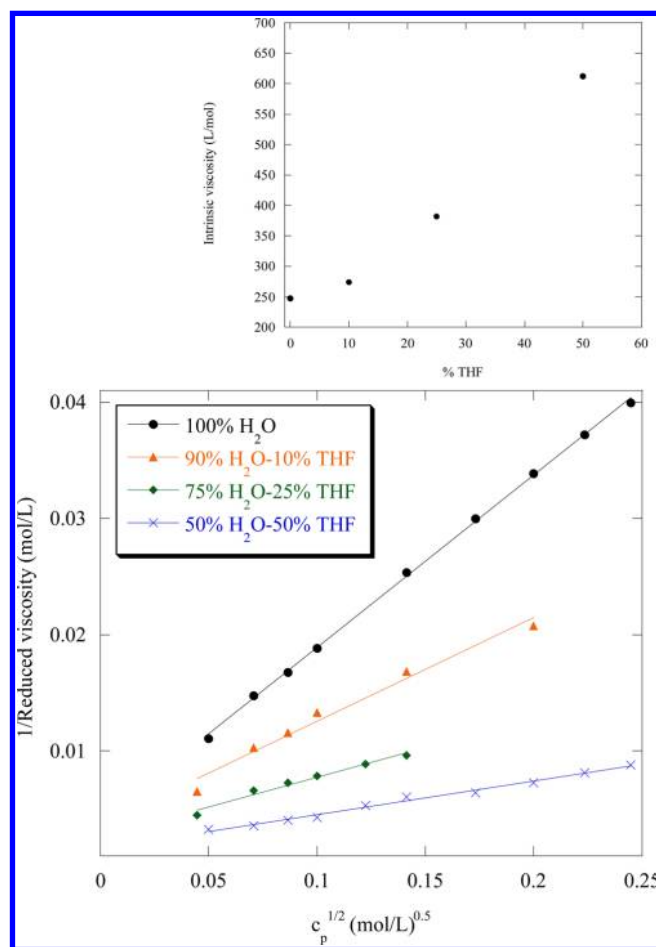


**Figure 11.** Fit of the viscometric data on PSS  $f = 0.38$  at 25 °C as a function of solvent composition with the Fuoss equation. The inset represents the evolution of the extrapolated intrinsic viscosity for PSS  $f = 0.38$  as a function of solvent composition.

time that the number of effective charges per polyelectrolyte chain  $Z$  increases with THF addition. This behavior is in agreement with the increase of the intrinsic viscosity. *Note that to our knowledge, this type of behavior (increase of the polyelectrolyte solution viscosity despite the decrease of the dielectric constant of the medium) is observed for the first time.*

**Comparison between Viscosity and Scattering.** Comparing results from the two techniques, the viscosity results for this hydrophobic polyelectrolyte are most of the case in perfect agreement with those of neutron scattering, showing that the hydrophobic polyelectrolyte evolves to a structure characteristic of more charged and elongated chains under THF addition: the “pearls” previously present in the chain vanish, the chain unfolds and stretches out. This increase of the polyelectrolyte solution viscosity is the more marked the lower the charge fraction  $f$ . So, the polyelectrolyte is less and less sensitive to THF addition when  $f$  increases, until for highly charged PSSNa ( $f = 0.75$ ), the evolution is reversed. Then the viscosity *decreases* with THF addition, like for AMAMPS, because for highly charged hydrophilic polyelectrolytes, water plus a large amount of THF becomes a bad solvent. In other words, on top of the effect of  $\epsilon$ , a stronger effect of solvent quality ( $\tau$ ) now takes place. For an intermediate value of  $f = 0.5$ , the variation (not shown here) with added THF is clearly present, but less pronounced: it is intermediate between the variations observed for  $f = 0.38$  and the one observed for  $f = 0.75$ .

## V. CONCLUSION

The main effect described in this paper is the influence of the improvement of the solvent quality, through the addition of THF, on the structure of the aqueous hydrophobic polyelectrolyte solutions both by small angle neutron scattering and by viscosity measurements. These methods appear complementary and show a fair correlation. The characteristics of the structure function of the aqueous hydrophobic polyelectrolyte solutions evolve with THF addition. For the rate of charge  $f = 0.5$  and  $0.38$ , the peak height decreases, the peak position increases and the scattered intensity at zero angle decreases with THF addition. These variations indicate that the polyelectrolyte chain conformation becomes a more stretched conformation, joining the classical hydrophilic polyelectrolyte behavior. This is accompanied by an increase of viscosity with THF addition. As the charge rate  $f$  increases, the hydrophobicity of the PSSNa polyelectrolyte decreases, and at a sufficient high charge rate, the structure function remains constant with THF addition.

A second effect is, however, observed for the two hydrophilic polyelectrolytes, AMAMPS and PSS  $f = 0.75$ , because the evolution is reversed: the viscosity decreases with THF addition for large THF contents (25% and more strikingly 50%). Neutron scattering for 50% THF appears profoundly modified for PSS  $f = 0.82$ . Adding THF makes the polyelectrolyte character vanish: the solvent ability to dissociate charges is now weaker. This can be explained by a change of the average dielectric constant but more generally the subtleties of the solvation process are involved under these conditions.

Finally, let us return to a third effect noticed at low  $q$ : it comprises the decrease of the low  $q$  upturn and the decrease of the plateau at the foot of the upturn. They are difficult to separate. However, the decrease of the foot plateau can be related to the theoretical behavior of  $S(q \rightarrow 0)$  for the solution, i.e., to the osmotic compressibility ( $\sim 1/f_{\text{eff}}$ ). The decrease suggests that  $f_{\text{eff}}$  increases, as also inferred from the polyelectrolyte peak characteristics. Considering the upturn itself, it is attributed to large scale inhomogeneities of electrostatic origin, but also of hydrophobic origin for  $f = 0.38$ . In this case more work is necessary to understand which parameter,  $\epsilon$  or  $\tau$ , is winning. Beyond this, the point we want to make is that there could be another relation between scattering and viscosity than the one discussed in the paper: these inhomogeneities responsible for the upturn could also play a role in viscosity. Therefore, as an extension of this work, it will be very interesting to measure the form factor of the PSSNa by the zero average contrast technique using neutron scattering, as a function of THF addition. ZAC allows us to measure the chain conformation with in principle no perturbation from the upturn. The effect of chain conformation on the viscosity can then be separated from the effect of chain aggregation. We will then be able to attribute the viscosity changes either to conformation or to aggregation.

## ■ ASSOCIATED CONTENT

### ● Supporting Information

Figures SI 1, SI 2, SI 3: Evolutions at large, medium, and small  $q$  of the SANS profiles with the percentage of added THF to aqueous solutions of PSSNa. (a) PSSNa  $f = 0.82$  (b) PSSNa  $f = 0.50$  (c) PSSNa  $f = 0.38$ . The polyelectrolyte concentration  $c_p$  is  $0.34$  mol/L. Figure SI 4: Evolution of the SANS profile of PSSNa  $f = 0.82$  in 50% D<sub>2</sub>O–50% THF,  $c_p = 0.34$  mol/L

showing two crossovers: one from a plateau regime to a slope of  $-1.5$ , second a change of slope from  $-1.5$  to approximately  $-1$ . Figure SI 5: Comparison of the SANS profiles of the solutions: PSSNa  $f = 0.82$ –0% THF<sub>d</sub>, PSSNa  $f = 0.50$ –50% THF<sub>d</sub> and PSSNa  $f = 0.38$ –50% THF<sub>d</sub>. This information is available free of charge via the Internet at <http://pubs.acs.org>.

## ■ AUTHOR INFORMATION

### Corresponding Author

\*W.E.: tel, +216 21 19 55 23; fax, +216 71 53 76 88; e-mail, [essafi.wafa@inrap.rnrt.tn](mailto:essafi.wafa@inrap.rnrt.tn). F.B.: tel, +33 1 69 08 62 10; fax, +33 1 69 08 82 61; e-mail, [francois.boue@cea.fr](mailto:francois.boue@cea.fr).

### Notes

The authors declare no competing financial interest.

## ■ ADDITIONAL NOTE

The lowest value recorded for  $S(q \rightarrow 0)_{\text{measur}}$  is  $2 \times 10^{-3} \text{ \AA}^{-3}$  for PSSNa  $f = 0.38$ , 50% THF (Figure 4 and Figure SI 3b in the Supporting Information). From eq 2 we calculate  $S(q \rightarrow 0)_{\text{estim}} = 0.034/160f_{\text{eff}} = 2 \times 10^{-4}/f_{\text{eff}}$ . One usually takes  $f_{\text{eff}} = 0.35$ , i.e., the Manning value  $a/l_b \sim a/\epsilon^2/ekT$  for water ( $\epsilon = 78$ ) and a unit length  $a = 2.2 \text{ \AA}$ . This leads to an estimate  $S(q \rightarrow 0)_{\text{estim}} \sim 6 \times 10^{-4} \text{ \AA}^{-3}$ . Introducing the value of  $\epsilon$  for 50% THF, the Manning ratio becomes twice larger, and  $S(q \rightarrow 0) \sim 1.2 \times 10^{-3} \text{ \AA}^{-3}$ . The measured value  $2 \times 10^{-3} \text{ \AA}^{-3}$  in the case of low  $f$  at high THF percentage is therefore not far from the predicted one, although still higher. This can be attributed to the remaining of the upturn.

## ■ REFERENCES

- (1) *Principles of Polymer Science and Technology in Cosmetics and Personal Care*; Goddard, E. D.; Gruber, J. V., Eds.; Marcel Dekker: New York, 1999.
- (2) Mc Cormick, C. L.; Bock, J.; Schults, D. N. In *Encyclopedia of Polymer Science and Engineering*, 2nd ed.; John Wiley and Sons: New York, 1989; Vol. 17, pp 730–84.
- (3) Bock, J.; Varadaraj, R.; Schultz, D. N.; Maurer, J. J. In *Macromolecular Complexes in Chemistry and Biology*; Dubin, P. L., Bock, J., Davies, R. M., Schultz, D. N., Thies, C., Eds.; Springer-Verlag: Berlin, 1994; p 33.
- (4) *Polymers as Rheology Modifiers*; Schultz, D. N.; Glass, J. E.; Eds.; Advances in Chemistry Series 462; American Chemical Society: Washington, DC, 1991.
- (5) *Hydrophilic Polymer, Performance with Environmental Acceptability*; Glass, J. E.; Eds.; Advances in Chemistry Series 248; American Chemical Society: Washington, DC, 1996.
- (6) Essafi, W.; Spiteri, M. N.; Williams, C. E.; Boué, F. *Macromolecules* **2009**, *42*, 9568–80.
- (7) Dobrynin, A. V.; Rubinstein, M.; Obukhov, S. P. *Macromolecules* **1996**, *29*, 2974–9.
- (8) Kantor, Y.; Kardar, M. *Europhys. Lett.* **1994**, *27*, 643–8.
- (9) Dobrynin, A. V.; Rubinstein, M. *Macromolecules* **1999**, *32*, 915–22.
- (10) Dobrynin, A. V.; Rubinstein, M. *Macromolecules* **2001**, *34*, 1964–72.
- (11) Witten, T. A.; Pincus, P. *Europhys. Lett.* **1987**, *3*, 315–20.
- (12) Rabin, Y. *Phys. Rev. A* **1987**, *35*, 3579–81.
- (13) de Gennes, P. G.; Pincus, P.; Velasco, R. M.; Brochard, F. J. *Phys. (Paris)* **1976**, *37*, 1461–73.
- (14) Dobrynin, A. V.; Colby, R. H.; Rubinstein, M. *Macromolecules* **1995**, *28*, 1859–71.
- (15) Barrat, J. L.; Joanny, J. F. In *Advances in Chemistry and Physics*; Prigogine, I., Rice, S. A., Eds.; Wiley: New York, 1996; X C IV and references therein.
- (16) Micka, U.; Holm, C.; Kremer, K. *Langmuir* **1999**, *15*, 4033–44.

- (17) Limbach, H. J.; Holm, C.; Kremer, K. *Europhys. Lett.* **2002**, *60*, 566–72.
- (18) Limbach, H. J.; Holm, C. J. *Phys. Chem. B.* **2003**, *107*, 8041–55.
- (19) Schweins, R.; Huber, K. *Macromol. Symp.* **2004**, *211*, 25–42.
- (20) Liao, Q.; Dobrynin, A. V.; Rubinstein, M. *Macromolecules* **2006**, *39*, 1920–38.
- (21) Essafi, W.; Haboubi, N.; Williams, C. E.; Boué, F. J. *Phys. Chem. B* **2011**, *115*, 8951–60.
- (22) Williams, C. E. In *Electrostatic Effects in Soft Matter and Biophysics*; Holm, C., Kekicheff, P., Podgornik, R., Eds.; NATO Science Series; Kluwer Academic Publishers: Dordrecht, 2001; Vol. 46, pp 487–586.
- (23) Baigl, D.; Sferazza, M.; Williams, C. E. *Europhys. Lett.* **2003**, *62*, 110–6.
- (24) Essafi, W.; Lafuma, F.; Williams, C. E. In *Macro-ion Characterization. From Dilute solutions to complex fluids*, Schmitz, K. S., Ed.; ACS Symposium Series 548; American Chemical Society: Washington, DC, 1994; pp 278–286.
- (25) Essafi, W.; Lafuma, F.; Williams, C. E. *J. Phys. II* **1995**, *5*, 1269–75.
- (26) Essafi, W.; Lafuma, F.; Baigl, D.; Williams, C. E. *Europhys. Lett.* **2005**, *71*, 938–44.
- (27) Aseyev, V. O.; Tenhu, H.; Klenin, S. I. *Macromolecules* **1998**, *31*, 7717–22.
- (28) Aseyev, V. O.; Klenin, S. I.; Tenhu, H.; Grillo, I.; Geissler, E. *Macromolecules* **2001**, *34*, 3706–9.
- (29) Schweins, R.; Lindner, P.; Huber, K. *Macromolecules* **2003**, *36*, 9564–73.
- (30) Goerigk, G.; Schweins, R.; Huber, K.; Ballauf, M. *Europhys. Lett.* **2004**, *66*, 331–7.
- (31) Nierlich, M.; Williams, C. E.; Boué, F.; Cotton, J. P.; Daoud, M.; Farnoux, B.; Jannink, G.; Picot, C.; Moan, M.; Wolff, C.; et al. *J. Phys. (Paris)* **1979**, *40*, 701–4.
- (32) Nierlich, M.; Boué, F.; Lapp, A.; Oberthür, R. *Colloid. Polym. Sci.* **1985**, *263*, 955–64.
- (33) Jannink, G. *Makromol. Chem., Macromol. Symp.* **1986**, *1*, 67–80.
- (34) Essafi, W.; Lafuma, F.; Williams, C. E. *Eur. Phys. J. B* **1999**, *9*, 261–6.
- (35) Heitz, C.; Rawiso, M.; Francois, J. *Polymer* **1999**, *40*, 1637–50.
- (36) Oosawa, F. M. *Polyelectrolytes*; Dekker: New York, 1971.
- (37) Manning, G. S. *J. Chem. Phys.* **1969**, *51*, 924–33–934–8.
- (38) (b) Combet, J.; Isel, F.; Rawiso, M.; Boué, F. *Macromolecules* **2005**, *38*, 7456–69. (a) Combet, J.; Rawiso, M.; Rochas, C.; Hoffmann, S.; Boué, F. *Macromolecules* **2011**, *44*, 3039–52 (b).
- (39) Spiteri, M. N. Ph.D. Thesis, Orsay, 1997. Spiteri, M. N.; Williams, C. E.; Boué, F. *Macromolecules* **2007**, *40*, 6679–91.
- (40) Baigl, D.; Ober, R.; Dan Qu, D.; Fery, A.; Williams, C. E. *Europhys. Lett.* **2003**, *62*, 588–94.
- (41) Dan Qu, D.; Baigl, D.; Williams, C. E.; Möhwald, H.; Fery, A. *Macromolecules* **2003**, *36*, 6878–83.
- (42) Chepelianskii, A. D.; Mohammad-Rafiee, F.; Trizac, E.; Raphaël, E. *J. Phys. Chem. B* **2009**, *113*, 3743–9.
- (43) Spiteri, M. N.; Boué, F.; Lapp, A.; Cotton, J. P. *Phys. Rev. Lett.* **1996**, *77*, 5218–20.
- (44) Kiryi, A.; Gorodyska, G.; Minko, S.; Jaeger, W.; Stepanek, P.; Stamm, M. *J. Am. Chem. Soc.* **2002**, *124*, 13454–62.
- (45) Kirwan, L. J.; Papastravou, G.; Borkovec, M. *Nano Lett.* **2004**, *4*, 149–52.
- (46) Gromer, A.; Rawiso, M.; Maaloum, M. *Langmuir* **2008**, *24*, 8950–3.
- (47) Waigh, T. A.; Ober, R.; Williams, C. E.; Galin, J. C. *Macromolecules* **2001**, *34*, 1973–80.
- (48) Boué, F.; Cotton, J. P.; Lapp, A.; Jannink, G. *J. Chem. Phys.* **1994**, *101*, 2562–8.
- (49) Fuoss, R. M.; Strauss, U. P. *J. Polym. Sci.* **1948**, *3*, 246–63.
- (50) Jousset, S.; Bellissent, H.; Galin, J. C. *Macromolecules* **1998**, *31*, 4520–30.
- (51) Makowski, H. S.; Lundberg, R. D.; Singhal, G. S. U.S. Patent 3 870 841, 1975 to Exxon Research and Engineering Co.
- (52) Baigl, D.; Seery, T. A. P.; Williams, C. E. *Macromolecules* **2002**, *35*, 2318–26.
- (53) Mc Cormick, C. L.; Chen, G. S. *J. Polym. Sci., Polym. Chem. Ed.* **1982**, *20*, 817–38.
- (54) Cotton, J. P. *Comment faire une calibration absolue des mesures de DNPA*; LLB Web site, www-llb.cea.fr.
- (55) Farnoux, B.; Boué, F.; Cotton, J. P.; Daoud, M.; Jannink, G.; Nierlich, M.; de Gennes, P. G. *J. Phys. (Paris)* **1978**, *39*, 77–86.
- (56) Dragan, S.; Miahai, M.; Ghimici, L. *Eur. Polym. J.* **2003**, *39*, 1847–54.
- (57) Renard, E.; Justice, J. C. *J. Solution Chem.* **1974**, *3*, 633–47.
- (58) Tong, Z.; Ren, B.; Gao, F. *Polymer* **2001**, *42*, 143–9.